

# Li-Beam Measurements of Edge Electron Density and Impurity on JET

P Breger, D Summers, Z A Pietrzyk<sup>1</sup>, B Viaccoz, J Vince.

JET Joint Undertaking, Abingdon, Oxfordshire, OX14 3EA, UK.

<sup>1</sup> CRPP, Lausanne, Switzerland.

**"This document is intended for publication in the open literature. It is made available on the understanding that it may not be further circulated and extracts may not be published prior to publication of the original, without the consent of the Publications Officer, JET Joint Undertaking, Abingdon, Oxon, OX14 3EA, UK".**

**"Enquiries about Copyright and reproduction should be addressed to the Publications Officer, JET Joint Undertaking, Abingdon, Oxon, OX14 3EA".**

# Li-Beam Measurements of Edge Electron Density and Impurity on JET

P Breger, D Summers, Z A Pietrzyk<sup>1</sup>, B Viacoz, J Vince.

JET Joint Undertaking, Abingdon, Oxfordshire, OX14 3EA, UK.

<sup>1</sup> CRPP, Lausanne, Switzerland.

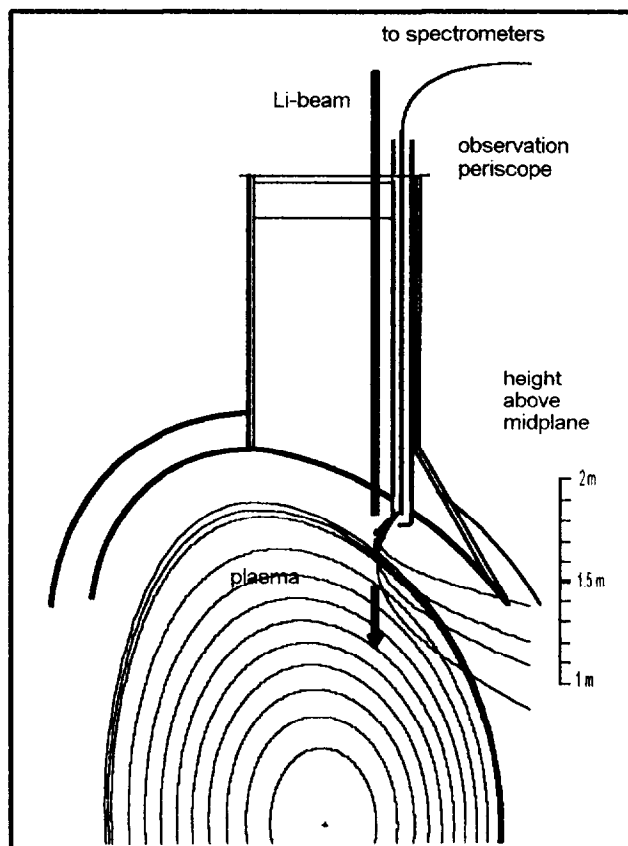
## INTRODUCTION

A Li-beam edge diagnostic has been implemented on JET. Employing a multifibre array and fast CCD cameras, beam emission and charge-exchange emission profiles can be obtained with high spatial and temporal resolution. Spectral resolution of the emission using spectrometers allows separate analysis of the various intrinsic plasma edge emissions in addition to the beam induced radiation. A new density deconvolution method has been developed to enable reconstruction of the density profile.

## DIAGNOSTIC LAYOUT

A 60 keV mono-energetic beam of neutral Li atoms is injected into the top edge region of the JET plasma near the stagnation point. An observation periscope is employed to monitor radiation emitted from a 17 cm section of the beam trajectory in the range 1.4 m to 1.85 m above the torus midplane. This is imaged onto a multi-fibre array (53 optical fibres, 1mm core diameter). The spatial resolution obtained is of order 4 to 7mm in radial direction. The density fall-off length in this region is of order 50 mm. The light is transported back to a diagnostic hall via fibres, where it is spectrally resolved and recorded by CCD detectors.

Fig. 1: Diagnostic Layout



## ION SOURCE

The ion source electrode geometry ( Fig. 2 ) is based on a modified Wehnelt extraction system [1], which has been optimised for JET using the source simulation code IONTRAK [2]. A Spectra-Mat emitter assembly (  $\varnothing$  15 mm ) is coated with ceramic  $\beta$ -Eucryptite (  $\text{Li}_2\text{O Al}_2\text{O}_3 \cdot 2(\text{SiO}_2)$  ). The extracted and focussed Li ion beam is neutralised in Li vapour. For commissioning purposes a Faraday cup can be inserted into the beam path at a distance of about 2m from the source. The operating voltages ( extraction and acceleration ), the emitter heating current and neutraliser temperature are optimised to yield maximum neutral beam intensity ( see Fig. 3 ).

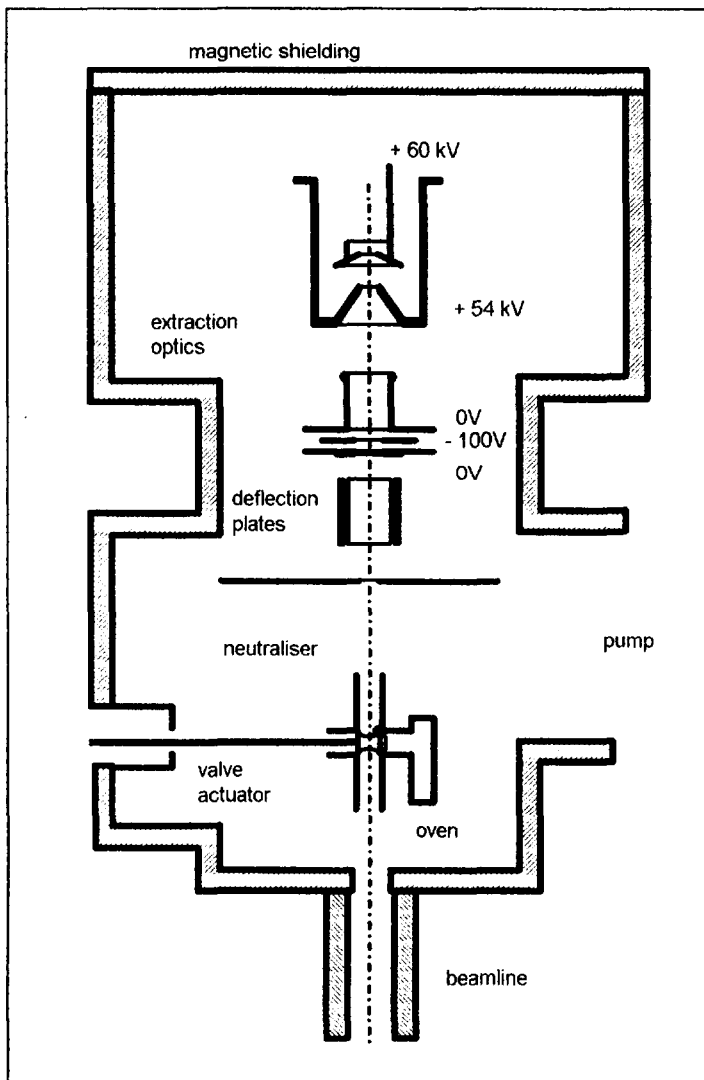


Fig. 2: Ion Source Setup

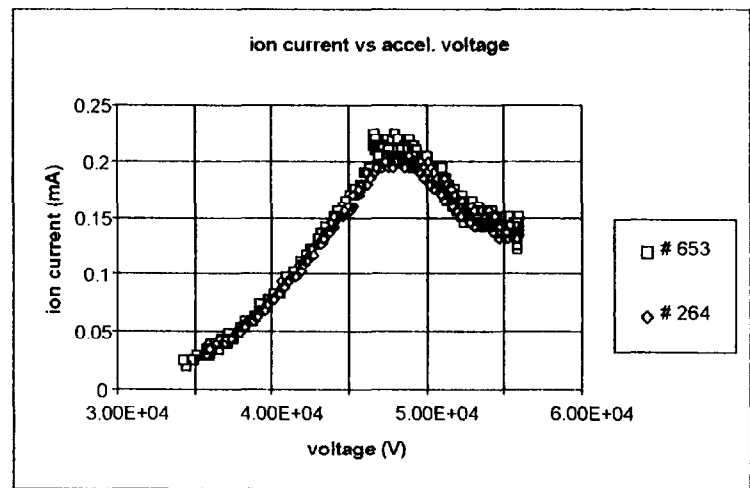


Fig. 3a: Optimisation of extracted ion current as function of acceleration voltage

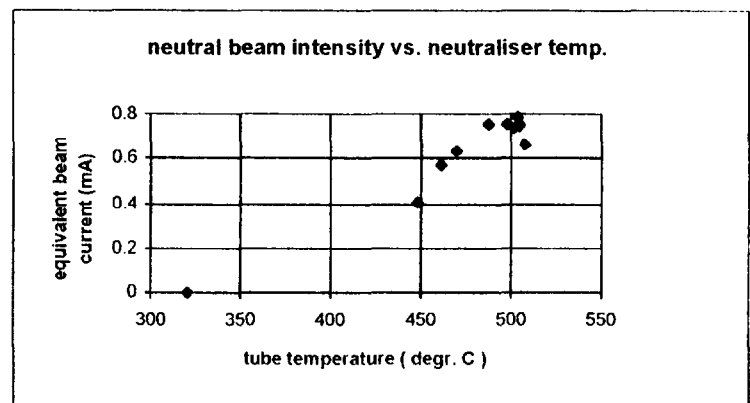


Fig. 3b: Beam current optimisation with respect to neutraliser temperature

## SPECTRAL ANALYSIS

53 optical fibres relay the light from the beam path to a diagnostic hall outside the biological shield. Four fibres are arranged to view the plasma next to the beam. These are used primarily for alignment purposes, but can also be used as a monitor of passive radiation from the plasma. 44 of the 53 fibres are imaged on the entrance slit of an astigmatism-corrected low-resolution spectrometer ( 0.27 m Chromex ) to separate the resonance beam emission at 670nm from the parasitic plasma background radiation. The resultant spatial profile of the beam emission can then be de-convoluted to obtain the **electron density profile** along the beam trajectory.

The remaining five beam monitoring fibres are passed to a high resolution spectrometer ( 1.25m SPEX ) to enable analysis of the beam induced impurity radiation ( charge-exchange radiation ) for **impurity density determination**.

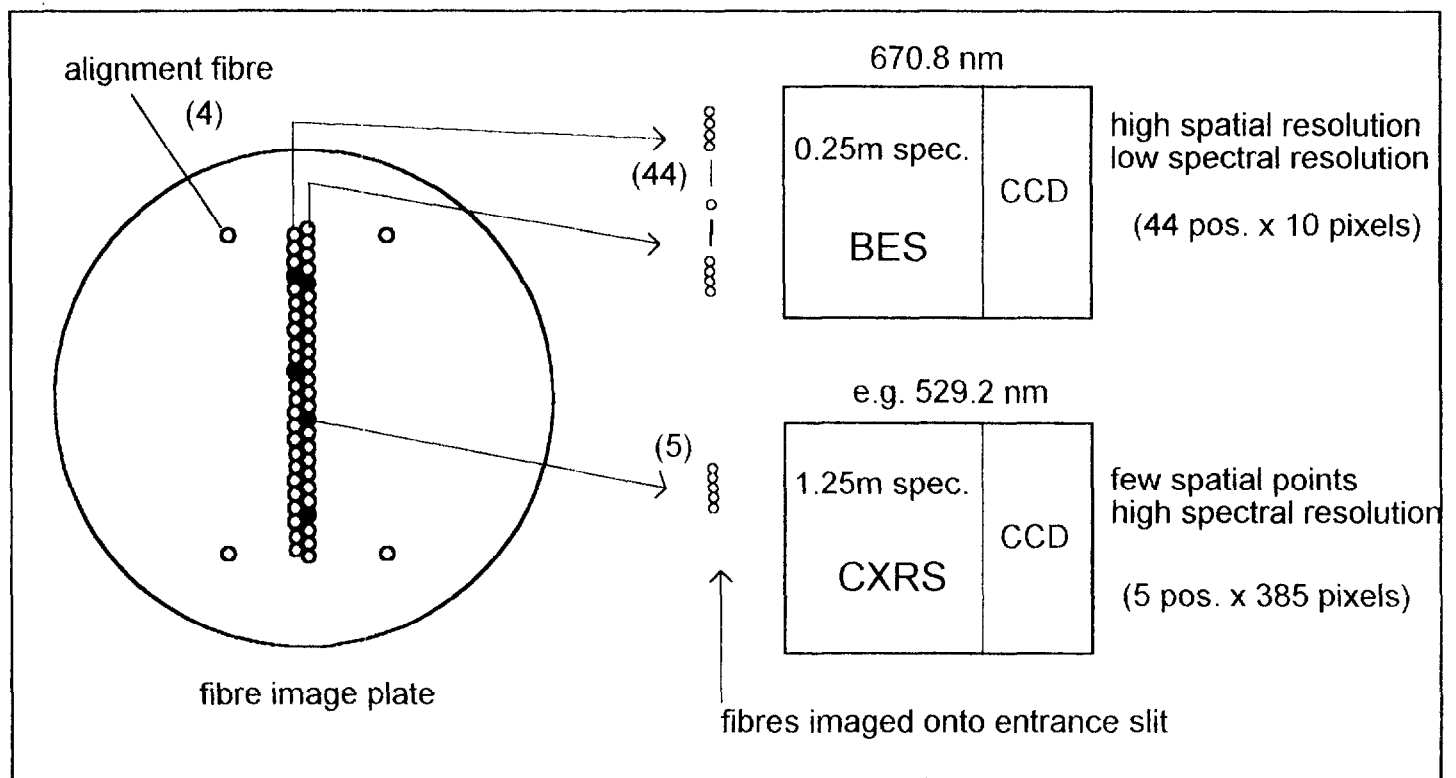


Fig. 4: Optical instrument layout.

For alignment purposes, the beam is injected into the torus filled with gas at a pressure of order  $10^{-5}$  mbar. The beam image at 670 nm is then recorded with both instruments ( see Fig. 5 ). The images on the CCD are Doppler-shifted due to different viewing line / beam intersection angles along the beam profile.

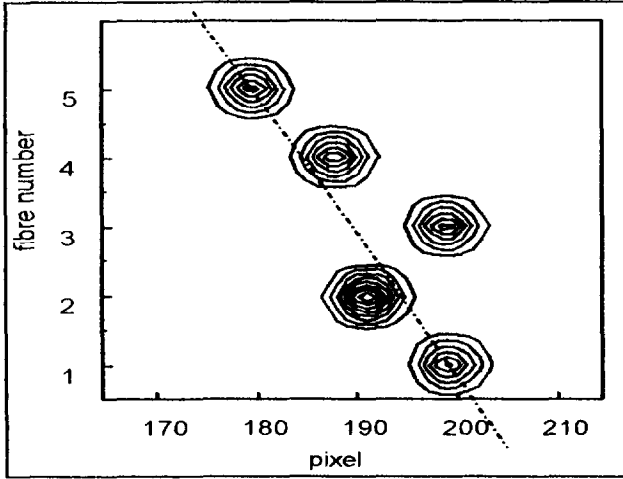


Fig. 5a: Fibre images on CXRS camera

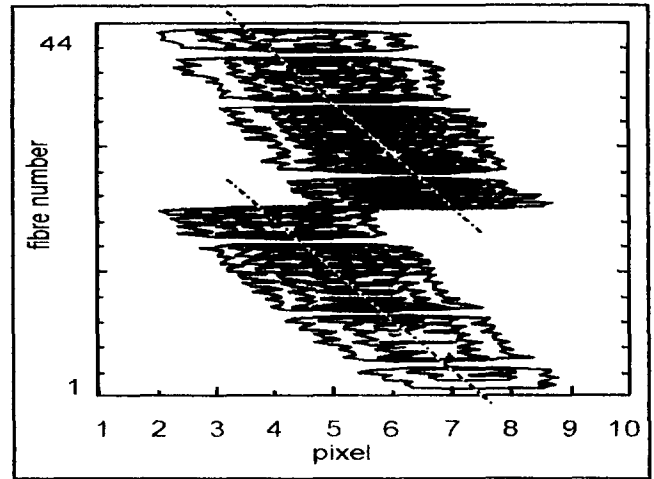


Fig. 5b: Fibre images on BES camera

The spatial position of the monitored beam profile in the torus is determined by two methods :

- back-illumination of the viewing lines with a laser and recording of the laser spots inside the torus with the in-vessel inspection system (IVIS)
- analysis of the Doppler-shift of the beam emission along the trajectory .

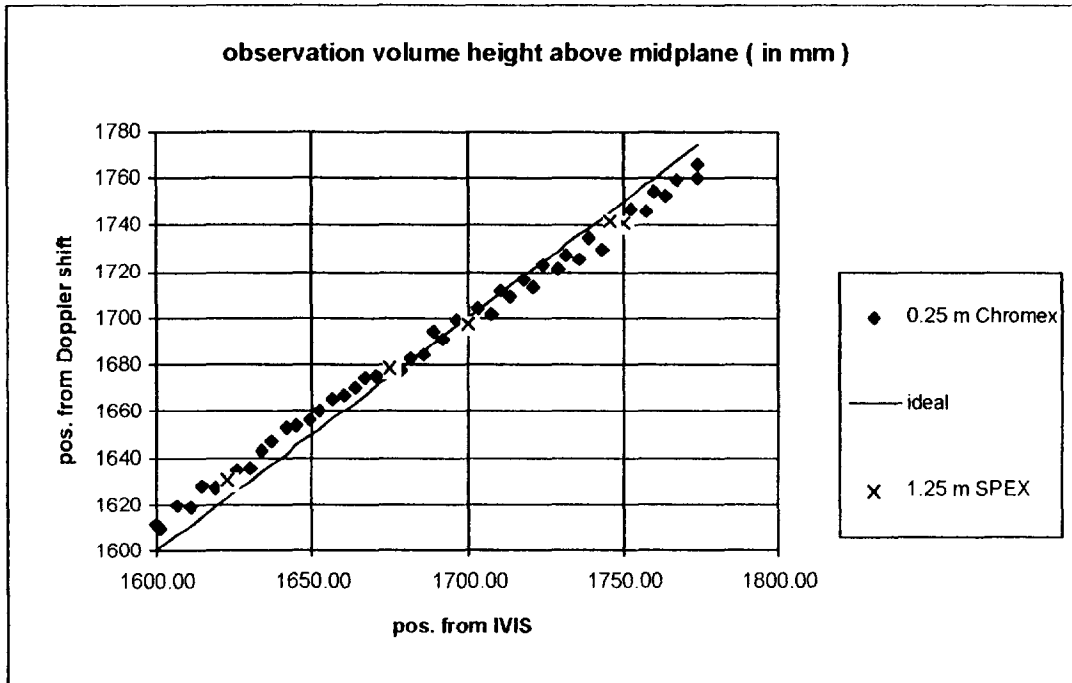


Fig. 6 : Comparison of in-vessel position of radial profile using two methods .

## ELECTRON DENSITY DETERMINATION

### Beam emission and attenuation model

The population of the Li-beam atomic levels ( $n_i$ ) is described by a coupled set of rate equations, which for a mono-energetic lithium beam can be written as :

$$\frac{dn_i}{dx} = \sum_{j=1}^n (n_e \cdot n_j \cdot a_{ij} + n_j \cdot k_{ij}) \quad (1)$$

The coefficients  $k_{ij}$  contain the spontaneous emission rates,  $a_{ij}$  contain the collision rates [4].

The observed line emission from the 2p - level is thus described by the population equation

$$\frac{dn_2}{dx} = n_e(x) \cdot \sum_{j=1}^n (n_j \cdot a_{2j}) + \sum_{j=1}^n (n_j \cdot k_{2j}) \quad (2)$$

### 'Normal' solution algorithm

From eq. 2 an *exact* expression for the local electron density  $n_e(x)$  can be calculated, which allows calculation of the electron density profile from the observed 2p-2s emission profile.

$$n_e(x) = \frac{\frac{dn_2}{dx} - \sum_{j=1}^n \left( \frac{n_j}{n_2} \cdot k_{2j} \right)}{\sum_{j=1}^n \left( \frac{n_j}{n_2} \cdot a_{2j} \right)} \quad (3)$$

This de-convolution algorithm is sensitive to :

- Limited experimental resolution (much worse than the numerical grid resolution used )
- Signal noise on emission profile ( affects differentiated profile sensitively )
- Absolute specification of the injected beam current
- Error in input plasma parameters of temperature, impurity content

- Singularity point instabilities - coefficients  $a_{ij}$  and  $k_{ij}$  can be positive or negative, depending on whether excitation or de-excitation is described. There exists a particular set of plasma conditions for which the numerator and denominator both can be equal to zero. This physically corresponds to the point where electron induced population of a level is equal to electron induced de-population. Since all electron collision rates are proportional to  $n_e$ , the value of  $n_e$  is undetermined at this point in the profile. Numerically, however, the point where denominator and numerator are equal to zero will not occur at the same grid point, causing singular behaviour in a deconvolution code.

To include proton and ion collisions in the model, the electron collision coefficients  $a_{ij}$  can be rewritten to include the diluted proton concentration and any impurity concentrations

$$a_{ij} \equiv a_{ij}^{el} + \left(\frac{n_p}{n_e}\right) \cdot a_{ij}^p + \left(\frac{n_C}{n_e}\right) \cdot a_{ij}^C + \left(\frac{n_{Be}}{n_e}\right) \cdot a_{ij}^{Be}$$

$$a_{ij}^k n_k \equiv \sum_{q=1}^{q_{max}} \frac{\langle \sigma_{k,q} v \rangle}{v_b} \cdot n_{k,q} = q_{k,rms}^2 \cdot \frac{\langle \sigma_p v \rangle}{v_b} \cdot n_k$$

This increases the requirement for atomic collision data as well as input data to the analysis code, but does not change the existence of a singularity point.

### 'Integral' solution algorithm [3]

To avoid the numerical difficulties around the singularity point, an integral form of eq. 2 can be used

$$n_2(x) = \int_z^x n_e(x) \cdot \sum_{j=1}^n (n_j a_{2j}) dx + \int \sum_{zj=1}^n (n_j k_{2j}) dx + n_2(z) \quad (4)$$

where  $z$  is the position at which the switch-over from the normal to the integral method is made. Integration by parts gives the formula used in the de-convolution code in the singularity region :



$$n_e(x) = \frac{n_2(x) + \int_z^x \frac{dn_e}{dy} \int_{z_j=1}^y \sum_{j=1}^n (n_j \cdot a_{2j}) dx dy - \int_{z_j=1}^x \sum_{j=1}^n (n_j \cdot k_{2j}) dx - n_2(z)}{\int_{z_j=1}^x \sum_{j=1}^n (n_j \cdot a_{2j}) dx} \quad (5)$$

## PREDICTED PERFORMANCE

The sensitivity of the proposed algorithm to the factors listed above has been investigated [3]. The numerical instability near the singularity is overcome successfully using the "integral method" in the critical region, and the "normal method" in the surrounding profile regions. The sensitivity to the experimental constraints are found to be acceptable

- reliable de-convolution is possible for experimental resolutions of 4mm
- using a suitable noise-reduction algorithm, de-convolution of density profiles with 25% statistical error was achieved in the presence of  $\pm 15\%$  noise
- the sensitivity on accurate specification of injected beam current is only critical near the singularity point in the profile - this can be exploited to calibrate the beam current
- the sensitivity to ion and electron temperature is small - 50% error in temperature results in density error  $< 10\%$
- the sensitivity on impurity specification is critical near the singularity point in the profile - 30% error in impurity specification results in density errors of about 15%, larger error in impurity concentration causes instabilities near singularity point

Presented below is an example calculation done on a simulated Li-beam emission measurement taking typical JET plasma conditions and the measured diagnostic sensitivity into account. The case shown corresponds to a 2.6 MA, 3.2 T plasma with neutral beam heating of 15 MW. The central electron density is  $4 \times 10^{19} \text{ m}^{-3}$ . The calibrated channel sensitivities and plasma positions were used to predict the Li 670 nm emission profile, shown in Fig. 7. The Li-beam parameters in the calculation were 1 mA equivalent intensity, and 60 keV beam energy. Superimposed on the calculated signal is a 10% noise (Poisson statistic). This signal has then been de-convoluted using above algorithm, the result is shown in Fig. 8.

The singularity point is at a position of 1.47 m (14.5 cm into the plasma profile), the separatrix position is estimated to be at 1.49 m.

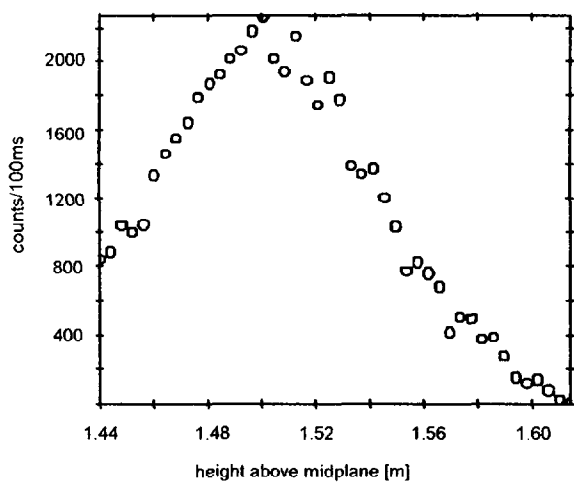


Fig. 7 : Simulated emission profile at 670 nm measured by CCD.

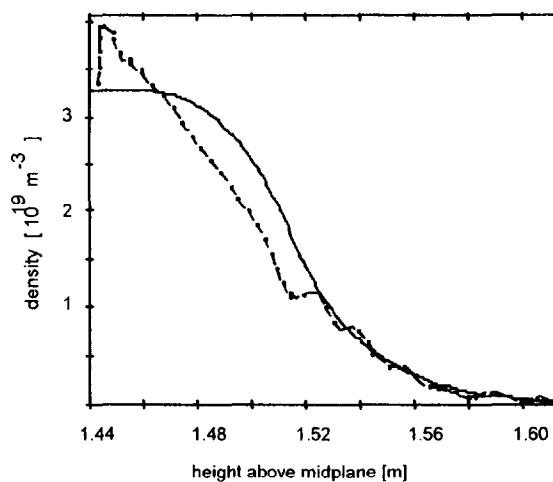


Fig. 8 : Comparison of de-convoluted density profile (dashed line) and original density profile used in simulation of Li-beam emission ( full line).

The de-convoluted density profile agrees well within the 25% error limit established previously for the diagnostic accuracy [3]. The large discrepancy at 1.52m is due to an unfavourable noise excursion in the emission profile, which cannot be distinguished from a real density perturbation.

## ACKNOWLEDGEMENTS

We should like to thank K.McCormick and J.Schweitzer for many helpful discussions, and the Swiss National Science Foundation for partially funding this work.

## REFERENCES

- [1] M Kick, K McCormick, H Schmid, A 100 keV neutral Lithium beam for plasma diagnostics, IPP Report IPP2/265, Max-Planck-Institute, Garching (1983)
- [2] A J T Holmes, S Norris, The IONTRAK Code, AEA Technology, Culham, Abingdon
- [3] Z A Pietrzyk, P Breger, D D R Summers , Plasma Phys. Control. Fusion **35** (1993) 1725-1744
- [4] F Aumayr et al, Atomic database for lithium beam edge plasma spectroscopy, IAEA report INDC-NDS-267 (1992)